Electronic Supplementary Information

Calorimetric and Spectroscopic Detection of Interaction Between a Diazo Dye and Human Serum Albumin

*Bhargav R. Patel and Kagan Kerman **

Dept. of Physical and Environmental Sciences, University of Toronto at Scarborough, 1265 Military Trail, Toronto, ON, M1C 1A4, Canada.

* Corresponding author

Email: *kagan.kerman@utoronto.ca*; Tel: +1-416-287-7250

Experimental

UV-visible spectroscopy

NanoDrop 2000c spectrometer (ThermoFisher Scientific, Mississauga, ON) was employed to study the UV-visible (UV-vis) absorption spectra of human serum albumin (HAS) in the presence and absence of Congo Red (CR) at 298 K in wavelength scanning mode across 200–700 nm, using PBS as a reference in a 1 cm quartz cell**.** The final dye and protein concentration were 2 µM each.

Fluorescence Microscopy

Non-functionalized polystyrene microspheres (10 µm) were purchased from Sigma-Aldrich (Oakville, ON). Polystyrene microspheres were passively adsorbed with HSA by incubating the microspheres in excess of HSA solution overnight. Fluorescence microphotographs of polystyrene beads adsorbed with HSA and complexed with CR were obtained using inverted EVOS FL (Life Technologies, Carlsbad, CA) epifluorescence microscope, equipped with LED light source. The fluorescent images were observed under x40 objective, using a QD655 light cube.

Results and Discussion

Study of HSA-CR Complex Formation Using Absorption Spectroscopy

Diligent analysis of the UV-vis absorption spectra of CR and HSA can assist in distinguishing the static and dynamic quenching mechanism.[1,2] During the dynamic quenching, the UV-vis spectra of HSA should superimpose, showing no changes, with the difference spectra of HSA-CR (i.e., subtracting the corresponding spectra of CR from HSA-CR). On the contrary, the static quenching produced due to the ground-state complex formation, will normally cause a modification in HSA's absorption spectrum.[1,3,4] UV-vis spectra of CR and HSA; in addition, the difference absorbance spectra of HSA-CR (1:1) were obtained to confirm the assumed static fluorescence quenching mechanism during HSA-CR interaction. As shown in Fig. S1, in the presence of CR, the UV-vis spectra of HSA displayed a shift in absorbance to lower wavelengths at around 280 nm. Thus, we concluded that the fluorescence quenching was primarily due to a ground-state complex formation during the HAS-CR interaction.[2]

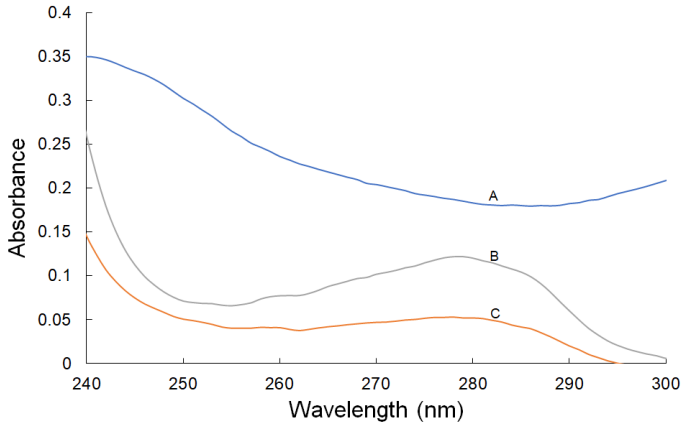

Fig. S1: UV–vis absorption spectra of CR, HSA, and difference spectra HSA–CR solutions; *c*(HSA) = *c*(CR) = 2 µM. (A) CR spectrum only; (B) HSA spectrum only; (C) the difference spectrum between CR–HSA and CR at the identical concentrations.

Determination of Association Constant and the Number of Binding Sites

Assuming CR fundamentally binds to identical and independent sites in HSA during the ground state complex, a modified Stern-Volmer equation[1,2,5] derived from the double logarithmic regression curve can be used to calculate the binding variables:

$$\log\frac{F_0 - F}{F} = \log K_a + n\log[Q] \qquad (1)$$

where, F_0 and F represents the fluorescence intensity without and with the CR, respectively. [Q] is the CR concentration. K_a is the association constant of interaction between CR and HAS, and n is the total binding sites on HSA for CR molecules. The binding sites (slope) and the association constant (Y-intercept) were determined from the linear regression graph of $\log(F_0-F)/F$ against log[Q]. The corresponding values of K_a and n at various temperatures are given in Table S1. The quenching experiments were performed at temperatures 298, 305, and 310K, because HSA was reported to show no structural degradation under those chosen conditions[6] and the temperatures were closer to the physiological conditions, under which CR might be interacting with HSA.

The results showed an antagonistic effect of different temperature values on K_a, where the values decreased with increasing temperature. This suggested that elevated temperatures caused instability and possibly resulted in the dissociation of the CR-HSA complex.[5] Moreover, static quenching mechanism was confirmed due to the observed decreasing trend during the interaction between CR and HSA.[2] Since the domain structure of HSA was very well elucidated[5,7], we hypothesised that the binding of CR in HSA occured at a site located near the sole tryptophan (Trp214) in HSA. In addition, the hydrophobic compartment of subdomain IIA (Sudlow's site 1) is proposed to be binding site for CR.[8] Therefore, the value of K_a is 1.10×10^8 $L.mol^{-1}$ at 298K, indicated that a high interaction existed between CR and HSA in the site around Trp-214. Also, the binding site value approximately equalled 1.38, which concluded that HSA had at least one independent class of high affinity binding for interaction with CR. The thermodynamic parameters were determined through a non-calorimetric approach - van't Hoff (eqn 2) and Gibbs−Helmholtz (eqn 3) equations - using the temperature dependent binding affinity values.

$$\ln K_a = -\frac{\Delta H}{RT} + \frac{\Delta S}{R} \quad (2)$$

$$\Delta G = \Delta H - T\Delta S \quad (3)$$

However, there are some drawbacks of a non-calorimetric approach to thermodynamics. The binding affinity and thermodynamic parameters from the fluorescence spectroscopy only considered local changes around the tryptophan (Trp-214) associated with resulting optical changes.[9–11]

Table S1: Binding and thermodynamic variables derived from the interaction of CR with HSA at various temperatures. Results are shown as mean ± S.D. (standard deviation) for experiments performed in triplicates (n=3)

T (K)	K_a ($L.mol^{-1}$)	n	ΔG ($kJ.mol^{-1}$)	ΔH ($kJ.mol^{-1}$)	ΔS ($J.mol^{-1}$)
298	$1.10\pm0.25 \times 10^8$	1.38±0.02	-45.92±0.55	-10.24±0.44	119.69±0.12
305	$1.02\pm0.63 \times 10^8$	1.38±0.05	-46.70±0.62		
310	$9.41\pm1.2 \times 10^7$	1.36±0.09	-47.36±0.63		

Isothermal Titration Calorimetry

Following equations were used determine the association constant, K_a, stoichiometric ratio, n, and the enthalpy change ΔH:[12]

$$K = \frac{\theta}{(1-\theta)[X]} \quad (4)$$

Where, θ = number of sites on HSA taken by CR and [X] = concentration of unbound CR. X_t representing the overall concentration, bound and unbound, of CR, was obtained by the following equation:[12]

$$X_t = [X] + n\theta M_t \quad (5)$$

where the total concentration of HSA in, V_{cell}, the active cell volume is represented by M_t. Q indicating the overall heat proportion of the solution in V_{cell} was derived by:[12]

$$Q = n\theta M_t \Delta H V_{cell} \quad (6)$$

Assuming the change in volume, ΔV_i, with i injection, the following equation was used to determine the heat absorbed or released ΔQ_i at i^{th} injection:[12]

$$\Delta Q_i = Q_i + \frac{\Delta V_i}{V_{cell}}\left[\frac{Q_i + Q_{(i-1)}}{2}\right] - Q_{(i-1)} \quad (7)$$

Gibbs free energy change and the entropy changes during the interaction were obtained using the equation below:

$$\Delta G = -RT \ln K_a = \Delta H - T\Delta S \quad (8)$$

where R was the gas constant (8.314472 J $K^{-1}mol^{-1}$) and T represents the temperature in K (298 K).

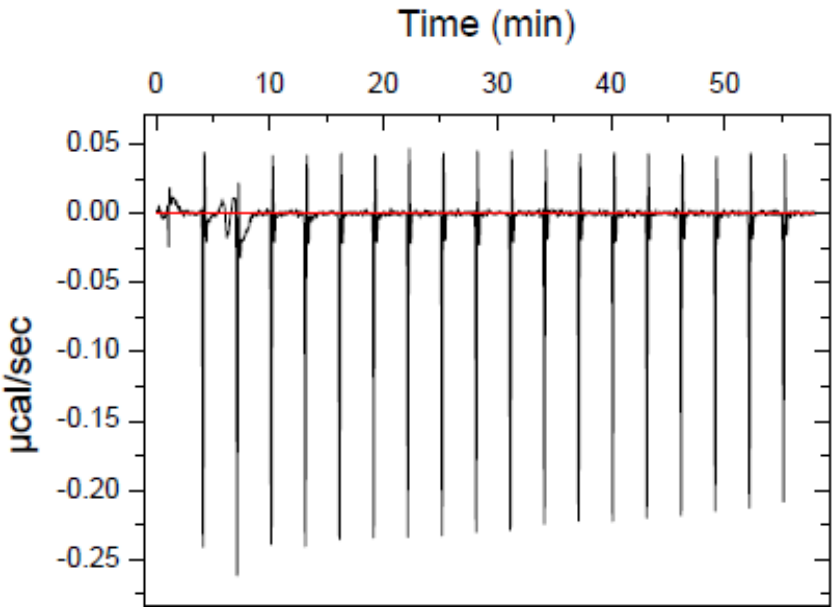

Fig. S2 (a): Interaction of 50% (v/v) human serum with 0.1 M PBS and target buffer through isothermal titration calorimetry at 298 K and pH 7.4. The thermal offset of the calorimeter required to maintain the sample and the reference cell at a constant temperature is referred to as the heat flow. The plot shows ITC thermogram for titration of 50% human serum (in syringe) with target buffer (in sample cell) that was used in the correction for heat of dilution.

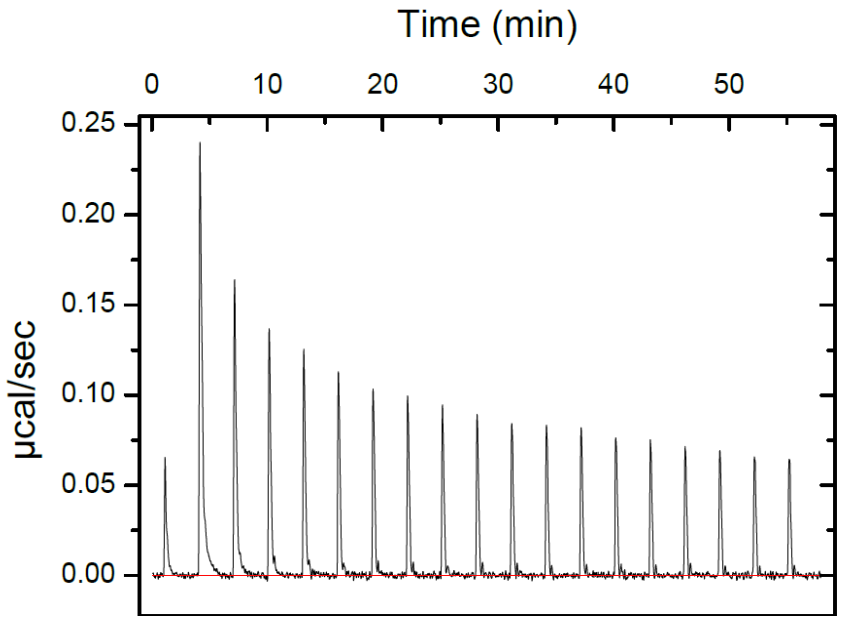

Fig. S2 (b): Interaction of 500 µM HSA and target buffer through isothermal titration calorimetry at 298 K and pH 7.4. The thermal offset of the calorimeter required to maintain the sample and the reference cell at a constant temperature is referred to as the heat flow. The plot shows ITC thermogram for titration of 500 µM HSA (in syringe) with target buffer (in sample cell) that was used in the correction for heat of dilution.

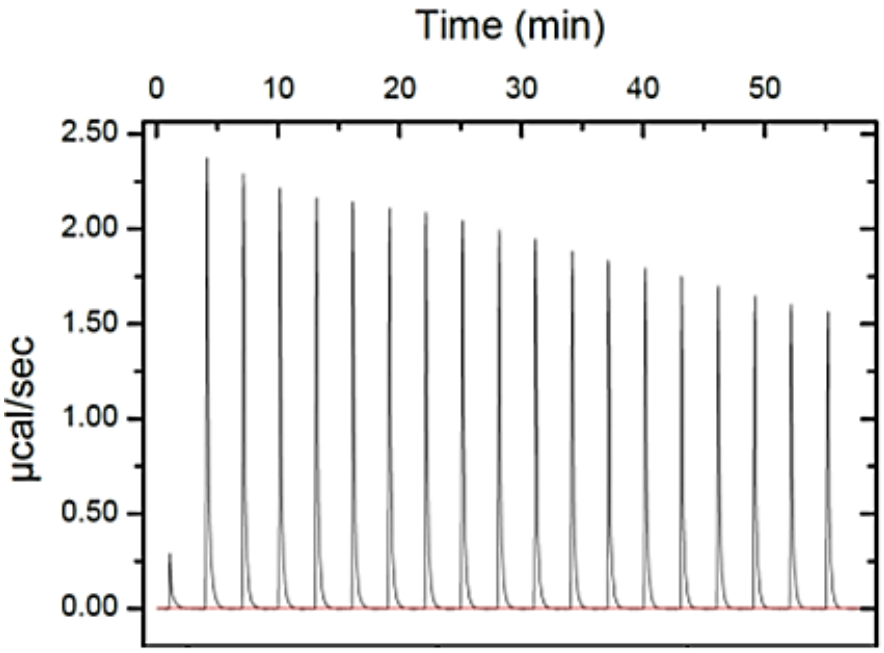

Fig. S2 (c): Interaction of 2.5 mM HSA and target buffer through isothermal titration calorimetry at 298 K and pH 7.4. The thermal offset of the calorimeter required to maintain the sample and the reference cell at a constant temperature is referred to as the heat flow. The plot shows ITC thermogram for titration of 2.5 mM HSA (in syringe) with target buffer (in sample cell) that was used in the correction for heat of dilution.

Study of HSA-CR Complex Formation Using Fluorescence Microscopy

Fluorescence microscopy is both simple and useful method for studying receptor-ligand binding interactions. According to the literature,[13] the wavelength for excitation and fluorescence emission of CR are 497 nm and 602 nm, respectively. Epifluorescence microscopy was used to observe the complexation between CR and HSA. Polystyrene microspheres (10 µm) that were passively adsorbed with HSA and incubated with CR overnight, were observed under an epifluorescence microscope (EVOS FL Cell Imaging System, Life Technologies, Carlsbad, CA) after rinsing. The emitted fluorescence from CR molecules that were bound to HSA upon excitation suggested an interaction with HSA (Fig. S3(a)) In the control experiments, polystyrene microspheres without the adsorbed HSA showed no fluorescence upon excitation indicating that the non-specifically adsorbed CR molecules were not detectable(Fig. S3(b)).

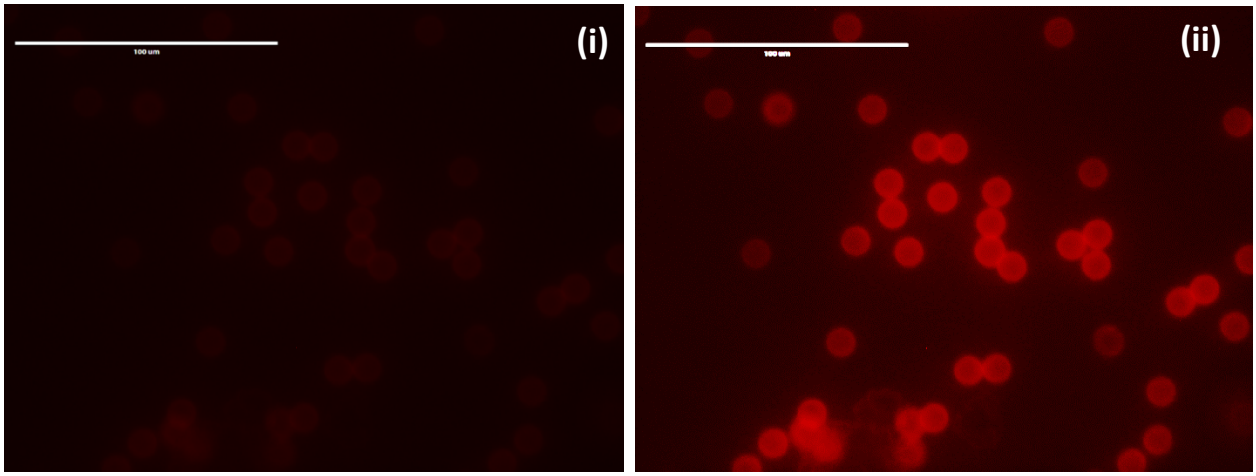

Fig. S3 (a): Fluorescence emission from polystyrene beads (10 µm) that were coated with HSA and then, incubated with CR under x40 magnification; Bar indicates 100 µm. Note: (i) Unmodified raw image, (ii) Image under +40% contrast and +60% brightness.

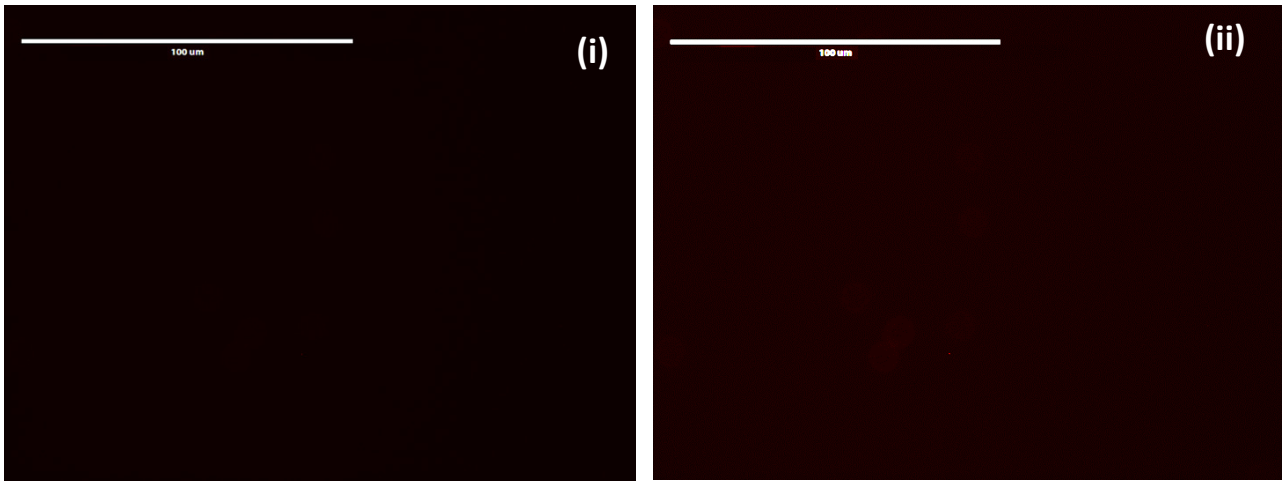

Fig. S3 (b): Fluorescence emission from polystyrene beads (10 µm) that were not coated with HSA prior to incubation with CR under x40 magnification; Bar indicates 100 µm. Note: (i) Unmodified raw image, (ii) Image under +40% contrast and +60% brightness

Competitive Binding Studies in the Presence of Site Markers: Chloroform and Ibuprofen

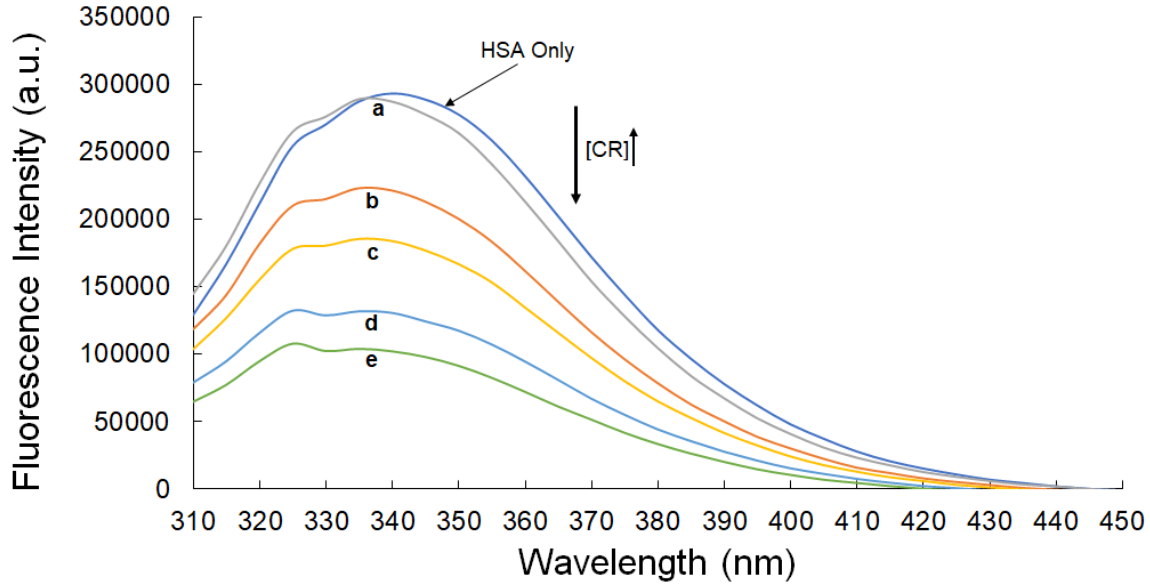

Fig. S4: Effect on the fluorescence intensity of 2 µM HSA in the presence of 2 µM chloroform upon additions of CR from 0-2 µM in (a) to (e) with increments of 0.50 µM. (T) 298 K, λ (ex) 295 nm.

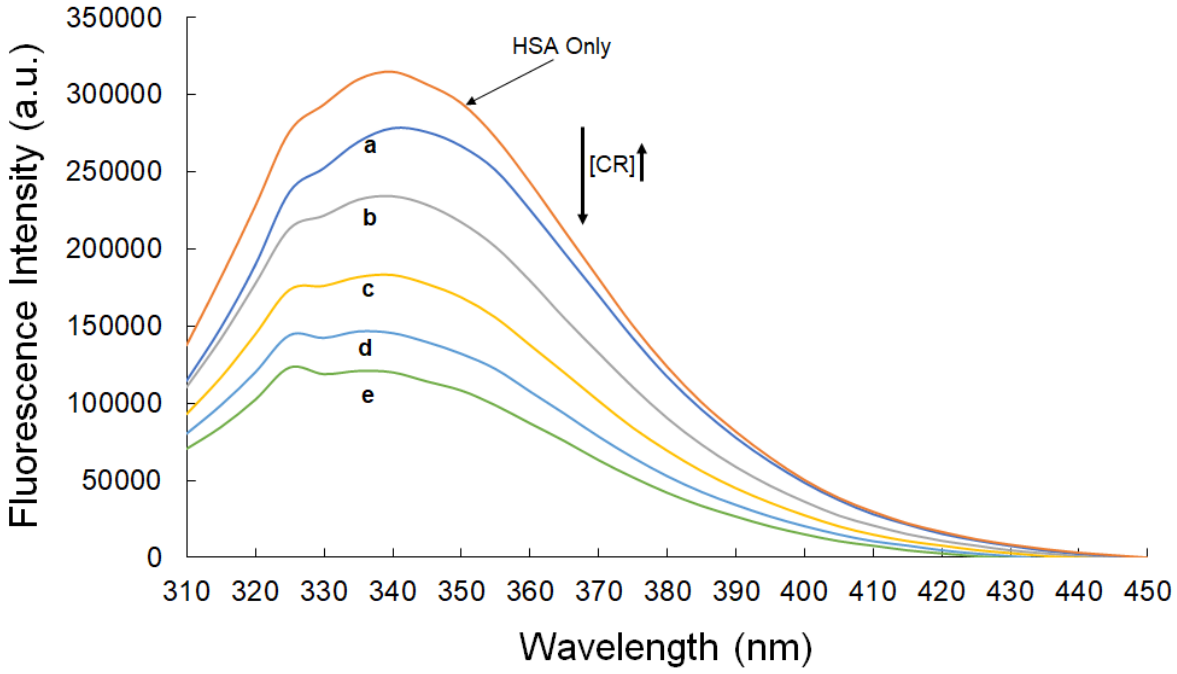

Fig. S5: Effect on the fluorescence intensity of 2 µM HSA in the presence of 2 µM ibuprofen upon additions of CR from 0-2 µM in (a) to (e) with increments of 0.50 µM. (T) 298 K, λ (ex) 295 nm.

References

1 Y.-J. Hu, Y. Ou-Yang, C.-M. Dai, Y. Liu and X.-H. Xiao, *Biomacromolecules*, 2010, **11**, 106–112.

2 Y.-Z. Zhang, X. Xiang, P. Mei, J. Dai, L.-L. Zhang and Y. Liu, *Spectrochim. Acta A Mol. Biomol. Spectrosc.*, 2009, **72**, 907–914.

3 A. S. Roy, *J. Biophys. Chem.*, 2010, **01**, 141–152.

4 J. R. Lakowicz, *Principles of Fluorescence Spectroscopy*, Springer US, NY, 3rd edn., 2006.

5 P. Bolel, N. Mahapatra and M. Halder, *J. Agric. Food Chem.*, 2012, **60**, 3727–3734.

6 M. Rezaei Tavirani, S. H. Moghaddamnia, B. Ranjbar, M. Amani and S. A. Marashi, *J. Biochem. Mol. Biol.*, 2006, **39**, 530–536.

7 S. Curry, H. Mandelkow, P. Brick and N. Franks, *Nat. Struct. Biol.*, 1998, **5**, 827–835.

8 A. K. Shaw and S. K. Pal, *J. Photochem. Photobiol. B Biol.*, 2008, **90**, 69–77.

9 T. Nada and M. Terazima, *Biophys. J.*, 2003, **85**, 1876–1881.

10 N. Zaidi, M. R. Ajmal, G. Rabbani, E. Ahmad and R. H. Khan, *PLoS One*, 2013, **8**, e71422.

11 R. Pattanayak, P. Basak, S. Sen and M. Bhattacharyya, *Biochem. Biophys. Reports*, 2017, **10**, 88–93.

12 A. Basu and G. Kumar, in *Natural and Artificial Flavoring Agents and Food Dyes, Volume 7*, eds. A. Grumezescu and A. M. Holban, Academic Press, London, 1st edn., 2018, pp. 133–164.

13 A. J. Veloso, H. Yoshikawa, X. R. Cheng, E. Tamiya and K. Kerman, *Analyst*, 2011, **136**, 4164–4167.